Chem. Pharm. Bull. **42**(12) 2598—2603 (1994) Vol. 42, No. 12

Fundamental Study on the Evaluation of Strength of Granular Particles

Kazumi DANJO,*[,a] Hironobu KATO,[b] Akinobu OTSUKA,[a] and Kouichi USHIMARU[b]

Faculty of Pharmacy, Meijo University,[a] 150 Yagotoyama, Tempaku-ku, Nagoya 468, Japan, Pharmacy Laboratories R & D Division, Nippon Shinyaku Co., Ltd.,[b] Nishiohji, Hachijo, Minami-ku, Kyoto 601, Japan.

Received June 8, 1994; accepted August 22, 1994

Compaction mechanisms and the strength required for compacting granular particles are considered to be influenced by granular particle strength. A fundamental study evaluating the crushing strength of particles by various methods was performed, and value obtained by the various methods were compared. Firstly, the particle diameter and crushing load for 140 particles were measured individually, and the single particle strength (σ_g) was calculated. The crushing strength exponentially decreased with an increase in particle diameter up to about 500 μm, and thereafter showed a constant value.

Next, the compression of multiple particles was measured. A linear relationship existed between the crushing load and the number of particles, and the average particle strength ($\bar{\sigma}_g$) was found to be lower than σ_g in every sample. This may be due to a variety of factors such as the distribution of particle diameter, shape, and crushing strength in multiple particles.

Finally, compaction tests of the particle bed were performed, and the parameters of some compression equations, which were recognized as values related to the particle strength were determined. The inflection points of the compression curve were also examined. The strength obtained from the first inflection point appeared to be in fairly good agreement with $\bar{\sigma}_g$.

Keywords compression test; compaction mechanism; crushing strength; particle diameter; particle strength; inflection point

Granular particle strength can be measured directly, where the particle crushing strength[1-3] is measured as the fracture load by which the particle is crushed, or indirectly ultilizing the crushing phenomena during the compression process of the powder bed. The physical aspect of the direct measurement method is clear; however, determination of a fracture load requires a great deal of time and labor, and always gives wide variations in results. Consequently, many particles must be tested to obtain a reliable result. Regarding the indirect measurement method, studies[4-7] of the relationship between particle strength and parameters in the equations of compression processes have enabled the deduction of average single particle and/or granular particle failure stress from simple uniaxial compression experiments. This indirect measurement method has obvious practical advantages, and the particle strength is measured from the inflection point of the compression curve.[8,9] However, some theoretical problems still remain. Ouwerkerk[10] discussed the "three strength test" which measures side crushing strength, bulk crushing strength and an annular shear test for spherical particles.

In this study, the average single particle strength obtained from measuring the crushing strength of one or ten spherical granular particles of Nonparel and the relatively large crystalline structure of methyl *p*-hydroxybenzoate were compared with respect to the failure stress of particles during compression of the powder bed.

Materials and Methods

Samples Spherical model granular particles comprised of 60—80% sugar and 20—40% cornstarch (Freunt Co., Ltd., Nonparel, NP) was used. Methyl *p*-hydroxybenzoate (Kanto Chemical Inc., MP) was recrystallized with ethyl alcohol and passed through an air jet sieve (Alpine Co., Ltd.). The physical properties of the samples are listed in Table I. Particle size and particle shape were determined using an image analyzer (Nireco, Luzex 500). Particle density for MP was measured with a helium-air pycnometer (Shimadzu-Micromeritics type 1302), and that for NP was calculated from the particle volume and the average particle weight using 1000 particles.

Measurement of Fracture Strength of Single Particles Single particle strength was measured with a hardness tester as shown in Fig. 1. The test particle was placed on an electronic balance plate and the rod was driven down at a speed of 0.14 mm/s until the particle was crushed. The weight needed to crush the particle (w) was measured by an electronic balance and the data were analyzed by a computer. Each measurement value shown is the average value of 100 particles.

The particle strength (σ_g) was calculated from the following equation[11]:

TABLE I. Physical Properties of Samples Used

Sample	Opening size (μm)	Mean particle diameter d_p (μm)	Particle density (g/cm^3)	Shape factor
NP-A	710—850	807	1.33	0.921
NP-B	500—710	648	1.29	0.894
NP-C	350—500	451	1.35	0.834
MP-A	710—1000	1079	1.37	0.654
MP-B	500—710	811	1.37	0.646
MP-C	350—500	523	1.37	0.642

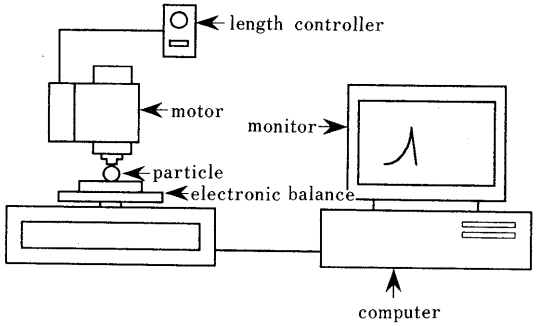

Fig. 1. Schematic Diagram of the Apparatus Used to Measure Particle Hardness

$$\sigma_g = 2.8w/(\pi d_p^2) \quad (1)$$

where w is the maximal load at the crushing of the particle, and d_p is the mean particle diameter.

Measurement of the Crushing Strength of Multiple Particles and of the Compression Load-Displacement Curve A multiple particle strength test was conducted using a universal tension and compression tester (Shimadzu, Autograph AG 5000D). Particles (number of particles, $n \leqq 100$) were compressed on an Autograph equipped with 16 mm flat face punches at a constant compressing speed of 0.5 mm/s, and the same equipment was used for the compression process of the powder bed.

Measurement of the Degree of Powdering The degree of powdering of the compressed NP was measured by passing the particles through 590, 420, and 300 μm sieves.

Measurement of Crushed Particle Numbers The number of crushed particles was measured by the tumbling-falling method as shown in Fig. 2. The particles were dropped onto a plastic plate with a rough surface set at a 5° angle. The plate was the vibrated by hand, and the number of crushed particles was calculated from the following equation:

number of crushed particles = (weight of the crushed particles that passed through the sieve + weight of the particles remaining on the plate − value of the blank)/(average weight of a particle) (2)

where the value of the blank is the weight of particles remaining in the same test before the compression test.

Results and Discussion

Fracture Strength of Single Particles Determination of the precise value of fracture strength of a single particle is now possible, and evaluation of the fracture strength in compressing a single particle has been generalized. However, fundamental information on the reliability of the method such that the effect of particle size and the number of particles that must be measured to obtain a reliable value is lacking. Therefore, we determined the particle sizes of NP (A, B, C) and measured the fracture strength of 140 of these particles. Figure 3 shows the distribution of particle sizes of NP in units of 10 μm.

Figure 4 is the typical compression load-displacement curve during the fracturing of a single particle of NP. The relationship between the particle diameter in units of 10 μm and the breaking load is shown in Fig. 5. The results indicated that the breaking load increased with increasing particle diameter.

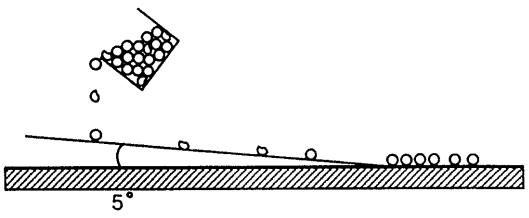

Fig. 2. Schematic Diagram of the Tumbling-Falling Method

Figure 6 shows the relationship between particle diameter and fracture strength as calculated from Eq. 1. The fracture strength decreased with increasing particle diameter until 500 μm, and about the same value remained for particles over 500 μm. It is well known that the fracture strength of a particle decreases almost exponentially with increasing particle diameter, according to the brittle fracture theory.[12] Our results conform to this theory up until a particle size of 500 μm.

The average breaking load ($\bar{w}$), average fracture strength (σ_g) and average fracture strength of a single particle (σ_g') calculated from average particle size and average breaking load are listed in Table II for NP-A, B, C. The average particle fracture strength, σ_g and σ_g' agreed closely with each other, and their values increased with a decreasing average particle diameter.

Evaluation of Crushing Strength of Multiple Particles To obtain an accurate value for the fracture strength of a single particle, many determinations are required. We examined the possibility of saving measurement time and labor by measuring the compression load-displacement curve and crushing strength of multiple particles, and compared the fracture strength obtained with that determined for single particles. Typical compression load-displacement curves for multiple NP-A particles are shown in Fig. 7. The peak observed at the comparatively lower displacement was recognized as the crushing point of the particles.

A linear relationship was observed between the particle number and compression load, as shown in Fig. 8. The average particle strengths, $\bar{\sigma}_g$, were determined from the slope of the straight line, and are listed in Table III. The values of $\bar{\sigma}_g$ obtained from multiple particles were lower than those of σ_g obtained from single particles. The lower value of $\bar{\sigma}_g$ may have been due to the distribution in particle size or strength in the multiple sample. Particles were not all crushed at the same time because of the particle distribution in the samples. Thus, the total crushing load of n particles is not always n times the crushing load of a single particle. However, $\bar{\sigma}_g$ is a characteristic value indicating the particle strength for a specified particle distribution because it is reproducible and is important in the compression of a powder mass.

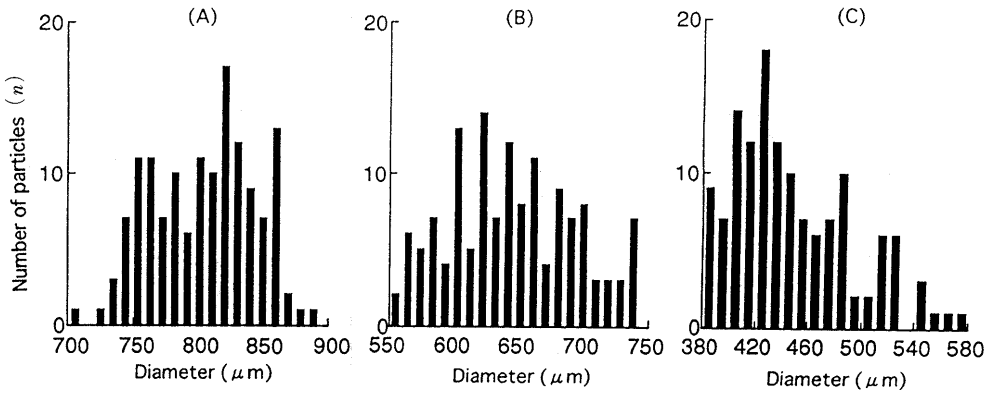

Fig. 3. Particle Diameter Distribution of NP

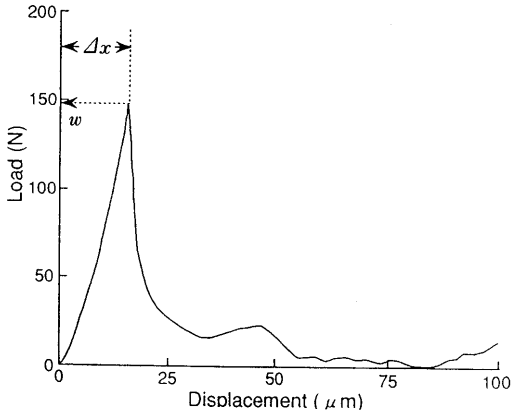

Fig. 4. Typical Compression Pattern of a Single NP Particle

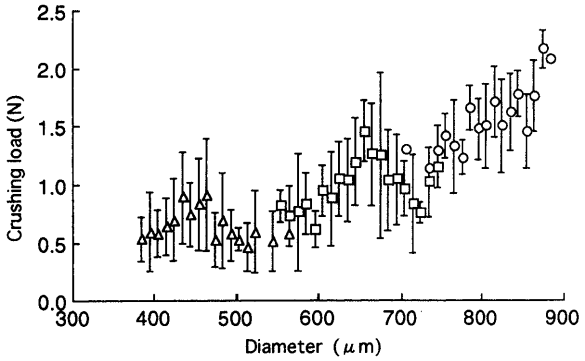

Fig. 5. Relationship between Particle Diameter and Crushing Load for NP

○, A; □, B; △, C. Each point represents the mean±S.D. for the particles shown in Fig. 3.

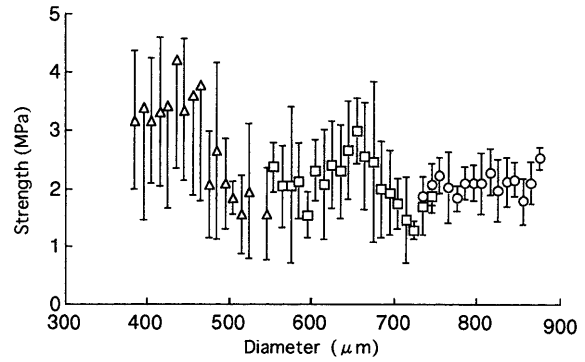

Fig. 6. Relationship between Particle Diameter and Strength of NP

○, A; □, B; △, C. Each point represents the mean±S.D. for the particles shown in Fig. 3.

The effects of particle size range, R, on the crushing load were examined by the following model examination. The particles were mixed with established particle size ranges, and the crushing loads were evaluated for $n=10$, 25 and 50, as shown in Fig. 9. The crushing load increased when the particle sizes were within a narrow range for each particle number. To make an exception of the effect of particle size range, we evaluated the average crushing strength, $\bar{\sigma}_g^*$, extrapolated to the zero value of the particle size range, and values of $\bar{\sigma}_g^*$ are shown in Table III. The value of $\bar{\sigma}_g^*$ was closer to the average crushing strength, σ_g, determined using a single particle, but the value still

TABLE II. Mechanical Properties Obtained by the Compression of a Single Particle

	$\bar{w}$ (N)	σ_g (MPa)	σ'_g (MPa)	$\Delta x^{a)}$ (μm)	Crushing$^{a)}$ energy ($\times 10^{-5}$ J)
NP-A	1.518	2.08	2.08	19.4	4.09
	(0.356)$^{b)}$	(0.44)		(4.53)	(1.04)
NP-B	1.025	2.19	2.18	16.7	6.08
	(0.378)	(0.81)		(4.40)	(2.81)
NP-C	0.656	2.99	2.87	13.0	2.18
	(0.321)	(1.57)		(3.80)	(0.98)
MP-A	0.761	—	0.93	—	—
	(0.358)				
MP-B	0.548	—	1.34	—	—
	(0.443)				
MP-C	0.404	—	1.99	—	—
	(0.319)				

a) Measured from the uniaxial compression pattern as shown in Fig. 4. *b*) Standard deviations are in parentheses. $\bar{w}$: average crushing load. σ_g: average particle strength calculated from the diameter and crushing load of individual oarticles. σ'_g: average particle strength calculated from the average diameter and crushing load. Δx: displacement until maximum breaking load.

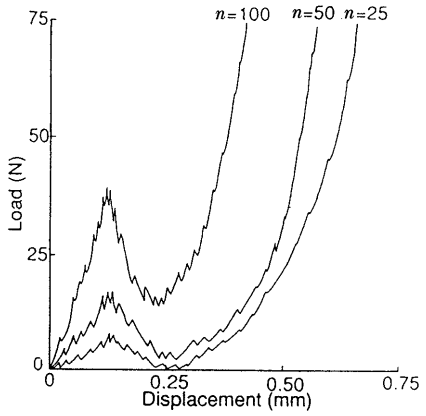

Fig. 7. Relationship between Load and Displacement in Multiple NP-A Particles

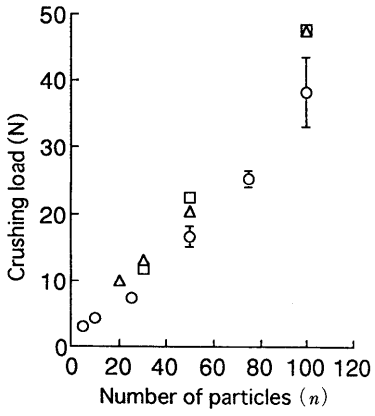

Fig. 8. Relationship between Number of Particles and Crushing Load for NP

○, A; □, B; △, C. Each point represents the mean±S.D. of 3 to 6 tests.

did not agree. From this result, we considered that not only particle distribution, but also the distribution of their internal structure, affected the maximum crushing load during the compression of a number of particles. However,

TABLE III. Average Granule Strength Obtained by the Compression Test of Multiple Particles

Sample	$\bar{\sigma}_g$ (MPa)	$\bar{\sigma}_g^*$ (MPa)
NP-A	0.49	0.80
NP-B	0.94	1.07
NP-C	1.64	2.21

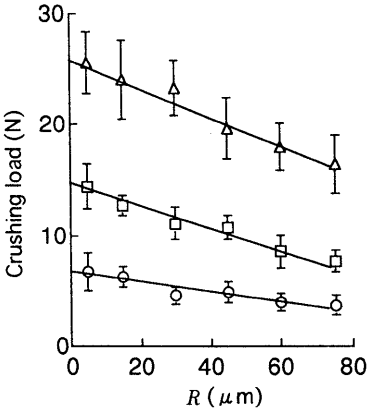

Fig. 9. Changes in Crushing Load with the Range of Particle Diameter in Sample (R) and Number of NP-A Particles (n)

○, $n=10$; □, $n=25$; △, $n=50$. Abscissa: ranges of mean particle diameters (R) Each point represents the mean ± S.D. of 3 to 6 tests.

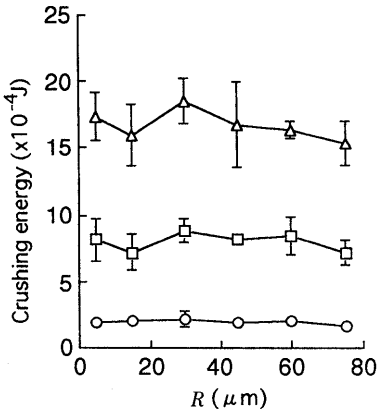

Fig. 10. Changes in Crushing Energy with Range of Particle Diameter in Sample (R) and Number of NP-A Particles (n)

○, $n=10$; □, $n=25$; △, $n=50$. Abscissa: same as in Fig. 9. Each point represents the mean ± S.D. of 3 to 6 tests.

the crushing energy was not significantly affected by particle distribution as shown in Fig. 10. For particle numbers of 25 and 50, the average crushing energy for n particles was close to n times that for a single particle (4.09×10^{-5} J). Therefore, the crushing energy obtained from the area under the compression load-displacement curve for a number of particles is a characteristic value indicating crushing resistance.

Evaluation of Particle Strength from the Compression Curve of the Powder Bed Many studies[13-16] on the evaluation of particle strength by compression of the powder bed have been reported. However, the relationship between the particle strength evaluated from the compression curve and the single particle strength has not been reported. We compared the results of particle strength

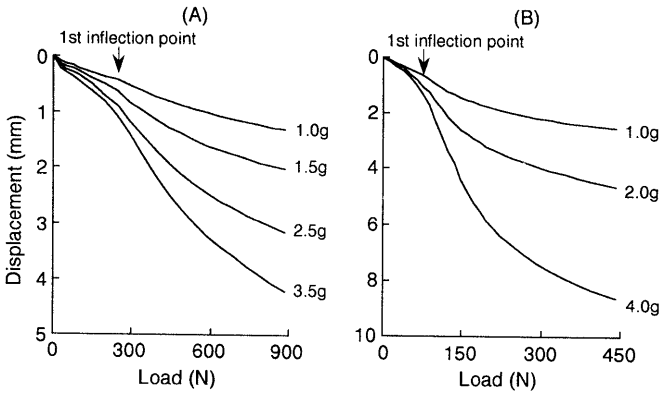

Fig. 11. Relationship between Compression Load and Displacement (A), NP-A; (B) MP-A.

evaluated from the compression curve with those of single or multiple particle strength.

Figure 11 shows the compression load and displacement curves for NP-A and MP-A. In these experiments, the punch was lowered gently onto the powder bed and stopped when the powder bed surface was touched. The displacement was then measured from this point. The figures show inflection points at the initial stage of the compression curves. For example, NP had an inflection point at about 200 N, and MP at about 70 N. These were considered the first inflection points, and were almost unchanged for samples from 1.0 to 4.0 g of powder weight. Kawakita[17] demonstrated the inflection points for glass beads, but did not show clearly the inflection points for powder particles. We attempted to explain our compression results according to Kawakita's and Heckel's equations as follows:

Kawakita's equation:

$$\gamma = abP/(1+bP) \tag{3}$$

$$P/\gamma = 1/(ab) + P/a \tag{4}$$

Heckel's equation:

$$-\ln \varepsilon = KP + A \tag{5}$$

where γ is the degree of volume reduction $=(V_0 - V)/V_0$, where V_0 is the initial volume and V is the volume at compression stress P, ε is the porosity of powder bed and a, b, and K are constants.

Figures 12 and 13 show the plots of the Kawakita's equation and Heckel's equation with 2.5 g of NP-A, B and C. Kawakita's plots showed a maximal value of P/γ ($P_{b,K}$) corresponding to the stress at the first inflection point. After this point, the value of P/γ decreased with increasing stress, and reached a minimal value ($P_{c,K}$) soon after P/γ, and stress, P, showed a linear relationship. Constants a and b of Kawakita's equation were obtained from the slope and tangent of this linear portion. On the other hand, for Heckel's plot, two inflection points were represented as shown in Fig. 13. That considered the first point was $P_{b,H}$ and the second point was $P_{c,H}$, and K_1 and K_2 were obtained from the slopes of the linear portions of each curve.

It is well known that the constants $1/b$ and $1/K$, which have dimensions of pressure, are related to the yield stress of individual powder particles. Kawakita[4] and Yamada[16]

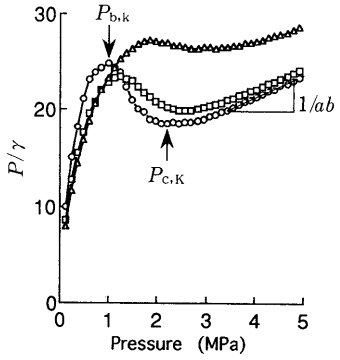

Fig. 12. Plots for NP Derived from Kawakita's Equation
○, A; □, B; △, C.

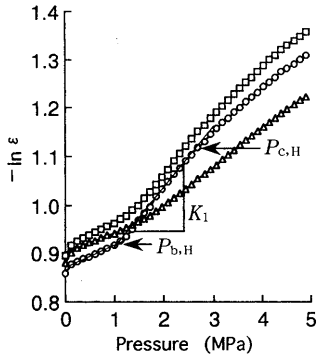

Fig. 13. Plots for NP Derived from Heckel's Equation
○, A; □, B; △, C.

reported that the yield strength, Y, and constant b gave the following relationship:

$$Y \fallingdotseq 2/(3b) \tag{6}$$

On the other hand, Y and constant K obtained by Heckel's plots gave the following relationship[6]:

$$Y \fallingdotseq 1/(3K) \tag{7}$$

We calculated the values of $2/(3b)$ and $1/(3K)$, and these are listed in Table IV. In this Table the values of $\sigma_{b,K}$, $\sigma_{b,H}$, $\sigma_{c,K}$ and $\sigma_{c,H}$ calculated by dividing $P_{b,K}$, $P_{b,H}$, $P_{c,K}$ and $P_{c,H}$ by the average particle number, N, in a horizontal section of the die, are also listed. The particle number was also calculated according to the Rumpf[18] and Otsuka[19] equation:

$$N = 6(1-\varepsilon)/(\pi d_p^2) \tag{8}$$

where d_p is the mean particle diameter and ε is the porosity of the powder bed.

It is interesting to compare the single particle strength with the particle strength obtained from the slope and inflection of the compression curves. In the present study, the particle strength obtained by the slope method was close to but somewhat larger than the single particle strength, σ_g, except the values of $1/(3K)_2$. Recently, Yamada *et al.*[7] reported a compression equation including the factor of particle strength, which combined Kawakita's and Rumpf's equations, and suggested that the value of $1/b$ is smaller than the value of $2/(3b)$ for hard and brittle

TABLE IV. Particle Strengths Obtained from Compression Test of Granule Bed (MPa)

Sample	Slope method[a]			Inflection point method[c]			
	$2/(3b)$	$1/(3K)_1$	$1/(3K)_2$[b]	$\sigma_{b,K}$	$\sigma_{b,H}$	$\sigma_{c,K}$	$\sigma_{c,H}$
NP-A	3.30	3.43	39.03	0.76	0.85	1.57	1.56
NP-B	3.63	3.82	44.02	0.92	0.94	1.76	1.79
NP-C	7.69	7.15	43.39	1.36	1.27	2.24	2.84
MP-A	0.85	1.00	12.78	0.18	0.22	0.66	0.69
MP-B	1.13	1.31	12.39	0.28	0.29	0.84	0.97
MP-C	2.09	1.77	12.54	0.27	0.40	0.92	1.12

a) Obtained from the slope of the linear portion of the plot in Figs. 12 and 13. *b*) Obtained from high pressure ranges. *c*) Obtained from the inflection points in Figs. 12 and 13.

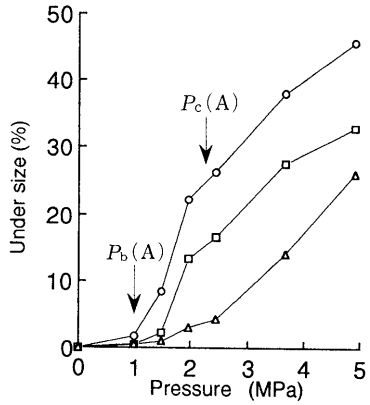

Fig. 14. Percent Under-Size after Compression of NP Particles
○, A; □, B; △, C. Pores of sieves, A, 590 μm; B, 420 μm; C, 300 μm.

particles. The NP and MP particles studied here may have these properties.

Next, we examined the particle strength evaluated from the inflection of the compression curve. Particle strengths, $\sigma_{c,K}$ and $\sigma_{c,H}$ obtained from the inflection point, P_c, were closely related to single particle strength, σ_g. This relationship has been reported previously Kuno[8]; however, the mechanism has not been clarified. On the other hand, the value of P_b was closely related to the initial breaking compression stress of the particle, $\sigma_{b,K}$, and the $\sigma_{b,H}$ values obtained from the breaking points were found to be 1/2—1/3 of σ_g. These small values were due to the fact that the values of $\sigma_{b,K}$ and $\sigma_{b,H}$ were calculated from the value of P_b divided by the average particle number, N, in horizontal sections.

It was necessary to check how the particles were broken during the compression process to evaluate the above observations. The particles removed from each compression process were passed through sieves and the results obtained for the NP-A—C samples are shown in Fig. 14. It was confirmed that the degree of powdering increased at the first inflection point for each sample. Crushing of particles likely occurred at this inflection point, as shown in Fig. 14.

Figure 15 shows the number of crushed particles measured by the tumbling-falling method, and the numbers of crushed particles at the first and second inflection points are listed in Table V. The calculated values were derived from Eq. 8.

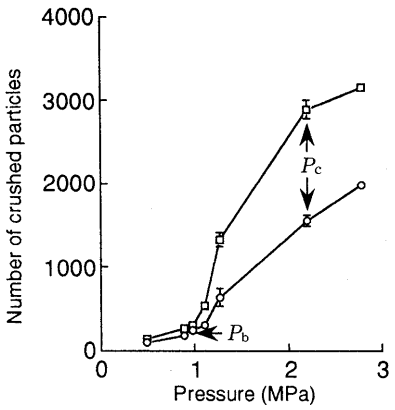

Fig. 15. Relationship between Compression Pressure and Number of NP-A Particles

○, 1.5 g of sample powder; □, 2.5 g of sample powder. Each point represents the mean ± S.D. of 5 tests.

TABLE V. Number of Particles at Inflection Points

	Weight of sample (g)	Calculation[a)]	Observation[b)]
1st inflection point	1.5	357	240
	2.5	353	301
2nd inflection point	1.5	387	1548
	2.5	385	2883

a) Calculated from Eq. 8. *b*) Measured by the tumbling-falling method.

The numbers of crushed particles obtained at the first inflection point were larger than the values calculated from Eq. 8. The value of σ_b calculated with this particle number was increased 1.5 times. On the other hand, at the second inflection point, quite a large number of particles were crushed, and the number of crushed particles was 4—10 times higher than the calculated values. Particle strength calculated with these values would thus be meaningless.

Determination of the particle strength calculated from the first inflection point, P_b, during the compression process suggested that the crushing of particles is related to average particle strength, $\bar{\sigma}_g$, as measured by the crushing of multiple particles. That is, the crushing phenomenon of particles crowded at the upper layer of the powder layer in the die is similar to the crushing of a number of particles on a plate. However, the particle strength measured by the inflection point method does not correspond with single particle strength, σ_g.

References

1) E. Horisawa, M. Yamada, K. Danjo, A. Otsuka, *Yakuzaigaku*, **52**, 13 (1992).
2) K. Danjo, *Pharm Tech Japan*, **9**, 81 (1993).
3) E. Horisawa, A. Komura, K. Danjo, A. Otsuka, *Chem. Pharm. Bull.*, **41**, 1428 (1993).
4) K. Kawakita, I. Hattori, M. Kishigami, *J. Powder Bulk Solid Technol.*, **1**, 3 (1977).
5) R. W. Heckel, *Trans. Metal. Soc. AIME*, **221**, 671 (1961).
6) R. W. Heckel, *Trans. Metal. Soc. AIME*, **221**, 1001 (1961).
7) N. Yamada, E. Abe, H. Hirosue, *Funtai Kougaku Kaishi*, **27**, 792 (1990).
8) H. Kuno, H. Imai, E. Abe, *Funtai To Funmatsu Yakin*, **33**, 111 (1986).
9) M. J. Adams, M. A. Mullier, J. P. K. Seville, *Powder Technol.*, **78**, 5 (1994).
10) C. E. D. Ouwerkerk, *Powder Technol.*, **65**, 125 (1991).
11) Y. Hiramatsu, Y. Okamoto, H. Kiyama, *Nippon Kogyo Kaishi*, **81**, 1024 (1965).
12) F. P. Knudsen, *J. Amer. Ceram. Soc.*, **42**, 376 (1959).
13) M. Duberg, C. Nystrom, *Powder Technol.*, **46**, 67 (1986).
14) P. V. Marshall, P. York, *Int. J. Pharm.*, **67**, 59 (1991).
15) N. Yamada, H. Hirosue, *Funtai Kougaku Kaishi*, **21**, 482 (1984).
16) N. Yamada, H. Hirosue, E. Abe, *Funtai Kougaku Kaishi*, **24**, 582 (1987).
17) K. Kawakita, A. Otsuka, Y. Tsutsumi, K. Danjo, Y. Okamoto, *Funtai To Funmatsu Yakin*, **12**, 116 (1965).
18) H. Rumpf, *Chemie-Ing. Tech.*, **42**, 538 (1970).
19) A. Otsuka, H. Sunada, K. Danjo, M. Nakagaki, *Yakugaku Zasshi*, **90**, 244 (1970).